IOP Publishing Phys. Scr. 97 (2022) 025503 https://doi.org/10.1088/1402-4896/ac437a

Physica Scripta

CrossMark

RECEIVED
25 July 2021

REVISED
1 December 2021

ACCEPTED FOR PUBLICATION
15 December 2021

PUBLISHED
17 January 2022

PAPER

Negative refractive index in a Doppler broadened three-level Λ-type atomic medium

Nguyen Van Ai, Nguyen Huy Bang and Le Van Doai*

Vinh University, 182 Le Duan Street, Vinh City, Vietnam

* Author to whom any correspondence should be addressed.

E-mail: doailv@vinhuni.edu.vn

Keywords: electromagnetically induced transparency, negative refractive index, doppler broadening

Abstract

We have achieved a negative refractive index with significantly reduced absorption in a three-level Λ-type atomic gas medium under Doppler broadening. It shows that the conditions for obtaining negative refractive index in the presence of Doppler broadening are very different from those of Doppler broadening absent. In particular, in order to obtain negative refractive index in the case of Doppler broadening the coupling laser intensity must be approximately ten times greater than that when the Doppler broadening is ignored. Meanwhile, the frequency band of negative refractive index with Doppler broadening is significantly expanded (about a hundred times) compared to that without Doppler broadening, however, the amplitude of negative refractive index decreases with increasing temperature (or Doppler width). Even in some cases as temperature (Doppler width) increases, the left-handedness of the material can disappear. In addition, we also show that the amplitude and the frequency band of negative refractive index can be changed by adjusting the intensity and the frequency of coupling laser. Our theoretical investigation can be useful for selection of laser parameters under different temperature conditions to achieve negative refractive index in experimental implementation.

1. Introduction

The refractive index is one of the important parameters that determine the optical properties of medium. From Maxwell's equations, the refractive index (n) of the medium is related to the relative permittivity (ε_r) and relative permeability (μ_r) through the relation $n^2 = \varepsilon_r \mu_r$. Therefore, the value of n can take either positive or negative root from this relation. For usual optical materials, both $\varepsilon_{\mathrm{r}} > 0$ and $\mu_{\mathrm{r}} > 0$ then $n = \sqrt{\varepsilon_r \mu_r}$ and the wave vector $\vec{k}$, the electric field $\vec{E}$ and the magnetic field $\vec{H}$ of the light form a right-handed system. In 1968, however, Veselago [1] first demonstrated theoretically that the medium also has simultaneously negative permittivity and permeability. For the medium with $\varepsilon_{\mathrm{r}} < 0$ and $\mu_{\mathrm{r}} < 0$ then $n = -\sqrt{\varepsilon_r \mu_r}$ and vectors $\vec{k}$, $\vec{E}$ and $\vec{H}$ of the light form a left-handed system. It is known as left-handed material (LHM) or negative index material (NIM) [1] and was experimentally verified a few years later [2, 3]. The negative index materials have become a hot topic of scientific research and attracted considerable attention in recent years due to their unusual electromagnetic properties and potential applications in many different fields [4–10].

Until now, several other methods have been proposed to achieve negative index material including artificial composite metamaterials [11], photonic crystal structures [12], transmission line simulation [13] and chiral media [14, 15]. However, these negative index materials usually occur in the high frequency range with accompanied strong absorption. Thus, the realization of negative index materials in the optical regime with small absorption is of great significance.

In recent years, negative refractive index has been realized in atomic gas media based on quantum interference and atomic coherence such as electromagnetically induced transparency (EIT) [16] and spontaneously generated coherence (SGC) [17]. This method has the following advantages: first, the negative

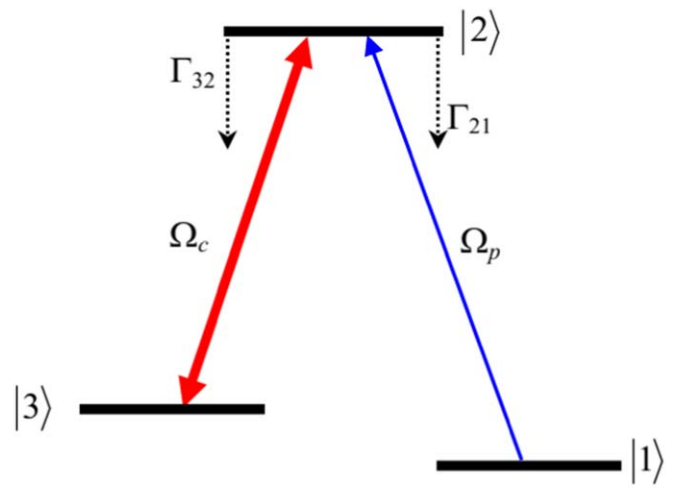

Figure 1. Three-level lambda-type atomic system is excited by the probe and coupling fields.

refractive index is easily obtained in the optical regime without absorption; second, the amplitude and the frequency band of the negative refractive index are also easily controlled by external fields. Using EIT effect, Oktel *et al* [18] and Shen *et al* [19] first proposed a scheme for realization of the negative refractive index in a three-level lambda-type atomic system. Later, Krowne *et al* [20] realized a negative refractive index using dressed-state mixed parity transitions of atom. Since then, several other studies on negative refractive index have been carried out in four- [21–26] and five- [27] level atomic systems that can be easily generated negative refractive index in different frequency bands. Recently, some authors have used the SGC effect to achieve negative refractive index with significantly reduced absorption and to control the frequency band of negative refractive index according to laser parameters and quantum interference parameter [28–30]. Under SGC condition, the refractive index can be switched from positive to negative or vice versa by varying the relative phase of laser fields and the strength of SGC.

The above studies on negative refraction in EIT materials have often ignored the Doppler effect and thus they can only be suitable for ultra-cooled atoms confined in a magneto-optical trap (MOT), for example. In order to be able to apply EIT materials in practice operating under different temperature conditions, some studies on EIT [31–37] as well as its applications such as group velocity [38–41], pulse propagation [42, 43], Kerr nonlinearity [44–47] and so on, have been included the Doppler broadening. It showed that the influence of Doppler broadening is very significant on the EIT effect at room temperature.

Although the negative refractive index in the three-level lambda system realized by Shen *et al* [19] under some ideal conditions such as the coupling laser beam is chosen to resonate with atomic transition and the Doppler effect due to the thermal motion of the atoms is ignored, and hence the relaxation processes between two sublevels of the ground state are also disregarded. However, for real atoms at room temperature, the conditions for achieving negative refractive index in this system can be very different. In this work, we present the realization of negative refractive index in Doppler broadened three-level lambda-type atomic system which is applicable to real atoms under different temperatures and therefore it may be useful for experimental implementation. The influences of Doppler width and coupling laser parameters on the refractive index of the medium for the probe laser are investigated.

2. Theoretical model

We consider a three-level lambda-type system as shown in figure 1, where $|1\rangle$ and $|3\rangle$ are two hyperfine levels of the ground state, while the level $|2\rangle$ is an excited state. In this case, the levels $|1\rangle$ and $|2\rangle$ have opposite parities, i.e., $\vec{d}_{21} = \langle 2|\ \hat{\vec{d}}|1\rangle \neq 0$ with $\hat{\vec{d}}$ is the electric dipole operator, whereas the two levels $|1\rangle$ and $|3\rangle$ have the same parities and $m_{31} = \langle 3|\ \hat{\vec{m}}|1\rangle \neq 0$ with $\hat{\vec{m}}$ is the magnetic dipole operator. Hence, the electric and magnetic components of the probe field with the same angular frequency ω_p can drive the transitions $|1\rangle \leftrightarrow |2\rangle$ and $|1\rangle \leftrightarrow |3\rangle$, simultaneously. Meanwhile, the transition $|3\rangle \leftrightarrow |2\rangle$ is linked by the strong coupling laser with the angular frequency ω_c. The frequency detunings of these laser fields are respectively defined by:

$$\Delta_p = \omega_p - \omega_{21},\ \ \Delta_c = \omega_c - \omega_{23}. \tag{1}$$

The Rabi frequencies of probe and coupling laser fields are related to their electric fields via the following relations:

$$\Omega_p = \frac{d_{21}E_p}{\hbar}, \tag{2a}$$

$$\Omega_c = \frac{d_{23}E_c}{\hbar}, \tag{2b}$$

with d_{mn} is the electric-dipole matrix element for the transition $|m\rangle$–$|n\rangle$; E_p and E_c represent the electric field envelope of the probe and coupling fields, respectively.

The density matrix equations of motion in the rotating-wave and electric dipole approximations are given as follows:

$$\frac{\partial\rho_{21}}{\partial t} = -(\gamma_{21} + i\Delta_p)\rho_{21} - \frac{i\Omega_p}{2}(\rho_{22} - \rho_{11}) + \frac{i\Omega_c}{2}\rho_{31}, \tag{3}$$

$$\frac{\partial\rho_{23}}{\partial t} = -(\gamma_{23} + i\Delta_c)\rho_{23} - \frac{i\Omega_c}{2}(\rho_{22} - \rho_{33}) + \frac{i\Omega_p}{2}\rho_{13}, \tag{4}$$

$$\frac{\partial\rho_{31}}{\partial t} = -[\gamma_{31} + i(\Delta_p - \Delta_c)]\rho_{31} - \frac{i\Omega_p}{2}\rho_{23} + \frac{i\Omega_c}{2}\rho_{21}. \tag{5}$$

where γ_{ij} is the coherence decay rate that related to the population decay rate Γ_{ij} by:

$$\gamma_{ij} = \frac{1}{2}\left(\sum_{k<i}\Gamma_{ik} + \sum_{l<j}\Gamma_{jl}\right), \tag{6}$$

Now we need to solve the system of equations (3)–(5) under the steady state condition $(\partial\rho/\partial t = 0)$ to find the solutions for ρ_{21} and ρ_{31} which related to the electric and the magnetic responses of the medium for the probe light. We assume that the atom initially populates in state $|1\rangle$, namely, $\rho_{11}^{(0)} \approx 1$, and $\rho_{22}^{(0)} \approx \rho_{33}^{(0)} \approx 0$. In the weak probe field regime, the solutions for ρ_{21} and ρ_{31} are given by

$$\rho_{21} = \frac{id_{21}E_p[\gamma_{31} + i(\Delta_p - \Delta_c)]}{2\hbar[(\gamma_{21} + i\Delta_p)[\gamma_{31} + i(\Delta_p - \Delta_c)] + \Omega_c^2/4]}, \tag{7}$$

$$\rho_{31} = -\frac{d_{21}E_p\Omega_c}{4\hbar[(\gamma_{21} + i\Delta_p)[\gamma_{31} + i(\Delta_p - \Delta_c)] + \Omega_c^2/4]}. \tag{8}$$

For an atomic gas medium, the electric susceptibility (χ_e) and the magnetic susceptibility (χ_m) are related to the density matrix elements by the following relations [19]:

$$\chi_e = \frac{2Nd_{21}}{\varepsilon_0 E_p}\rho_{21}, \tag{9}$$

$$\chi_m = \frac{2Nm_{31}}{H_p}\rho_{31} = \frac{2Nm_{31}}{\sqrt{\varepsilon_r\varepsilon_0/\mu_r\mu_0}\,E_p}\rho_{31}, \tag{10}$$

where N denotes the atomic density, d_{21} and m_{31} are respectively the electric and magnetic dipole matrix elements, H_p denotes the magnetic field envelope of the probe field with $H_p = \sqrt{\varepsilon_r\varepsilon_0/\mu_r\mu_0}\,E_p$, ε_0 and μ_0 are the permeability of vacuum.

Substituting (7) into (9) and (8) into (10), we obtain:

$$\chi_e = \frac{iNd_{21}^2}{\varepsilon_0\hbar}\frac{\gamma_{31} + i(\Delta_p - \Delta_c)}{[\gamma_{21} + i\Delta_p][\gamma_{31} + i(\Delta_p - \Delta_c)] + \Omega_c^2/4}, \tag{11}$$

$$\begin{aligned}\chi_m &= \frac{2Nm_{31}}{c\varepsilon_0 E_p}\sqrt{\frac{(1 + \chi_m)}{(1 + \chi_e)}}\rho_{31}\\ &= \frac{im_{31}}{2cd_{21}}\sqrt{\frac{(1 + \chi_m)}{(1 + \chi_e)}}\left(\frac{\Omega_c}{\gamma_{31} + i(\Delta_p - \Delta_c)}\right)\chi_e,\end{aligned} \tag{12}$$

with $c = 1/\sqrt{\varepsilon_0 \mu_0}$ is the speed of light in vacuum. Equation (12) has the solutions as:

$$\chi_m^{\pm} = \frac{-F^2 \pm \sqrt{F^4 - 4F^2}}{2}, \tag{13}$$

where

$$F = \frac{\chi_e}{\sqrt{1 + \chi_e}} \left(\frac{m_{31}}{2cd_{12}} \frac{\Omega_c}{\gamma_{31} + i(\Delta_p - \Delta_c)} \right). \tag{14}$$

In the above calculations, we have assumed the atoms are at rest. However, at room temperature the atoms will move with quite high velocities, so it is necessary to include the Doppler effect in the expressions of the electric susceptibility (χ_e) and the magnetic susceptibility (χ_m). In the experiment, to eliminate the first-order Doppler effect for the lambda-type configuration, the probe beam and the coupling beam are usually arranged to propagate in the same direction into the atomic medium. In this arrangement, when an atom moves with velocity v in the direction of the laser beams it will see an up-shift frequencies of the probe and coupling lasers as $\omega_p + (v/c)\omega_p$ and $\omega_c + (v/c)\omega_c$, respectively. Thus, the frequency detunings of the probe and coupling laser beams are changed to be $\Delta_p \to \Delta_p + (v/c)\omega_p$ and $\Delta_c \to \Delta_c + (v/c)\omega_c$, respectively. Considering the atoms moving along the axis of the laser beams, then the atomic velocity distribution follows the Maxwell distribution:

$$N(v) = \frac{N_0}{u\sqrt{\pi}} e^{-v^2/u^2} dv, \tag{15}$$

where $u = \sqrt{2k_B T/m}$ is the square root of the atomic velocity and N_0 is total atomic density.

In this way, the Doppler effect can be included in the expression of the electric susceptibility as

$$\chi_e(v)dv = \frac{id_{21}^2}{\varepsilon_0 \hbar u \sqrt{\pi}} \frac{N_0 e^{\left(-\frac{v^2}{u^2}\right)} dv}{\gamma_{21} + i\Delta_p + i\frac{\omega_p}{c} v + \dfrac{\Omega_c^2/4}{\gamma_{31} + i(\Delta_p - \Delta_c) + i\dfrac{(\omega_p - \omega_c)v}{c}}} dv. \tag{16}$$

Set $v^2/u^2 = x^2$ and omit the small term $i\frac{v}{c}(\omega_p - \omega_c)$ since the probe and coupling beams are close in frequency, therefore the expression (16) becomes

$$\chi_e(x)dx = \frac{iN_0 d_{21}^2}{\varepsilon_0 \hbar} \frac{e^{-x^2} dx}{\sqrt{\pi}\left(\dfrac{\omega_p u}{c}\right)\left[\dfrac{c}{\omega_p u}\left(\gamma_{21} + i\Delta_p + \dfrac{\Omega_c^2/4}{\gamma_{31} + i(\Delta_p - \Delta_c)}\right) - ix\right]}, \tag{17}$$

After integrating with respect to x from $-\infty$ to $+\infty$, the expression of the electric susceptibility in the presence of Doppler broadening as:

$$\chi_e(D) = \frac{iN_0 d_{21}^2 \sqrt{\pi}}{\varepsilon_0 \hbar \left(\dfrac{\omega_p u}{c}\right)} [e^{h^2}(1 - erf(h))], \tag{18}$$

where

$$h = \frac{c}{\omega_p u}\left(\gamma_{21} + i\Delta_p + \frac{\Omega_c^2/4}{\gamma_{31} + i(\Delta_p - \Delta_c)}\right), \tag{19}$$

and $erf(h)$ is the error function in the integral of the normalized Gauss function,

$$erf(h) = \frac{2}{\sqrt{\pi}} \int_0^h e^{-t^2} dt. \tag{20}$$

From there, we can easily find the expression of the magnetic susceptibility in the presence of Doppler broadening as

$$\chi_m^{\pm}(D) = \frac{-F^2(D) \pm \sqrt{F^4(D) - 4F^2(D)}}{2}, \tag{21}$$

where

$$F(D) = \frac{\chi_e(D)}{\sqrt{1 + \chi_e(D)}} \left(\frac{m_{31}}{2cd_{21}} \frac{\Omega_c}{\gamma_{31} + i(\Delta_p - \Delta_c)} \right). \tag{22}$$

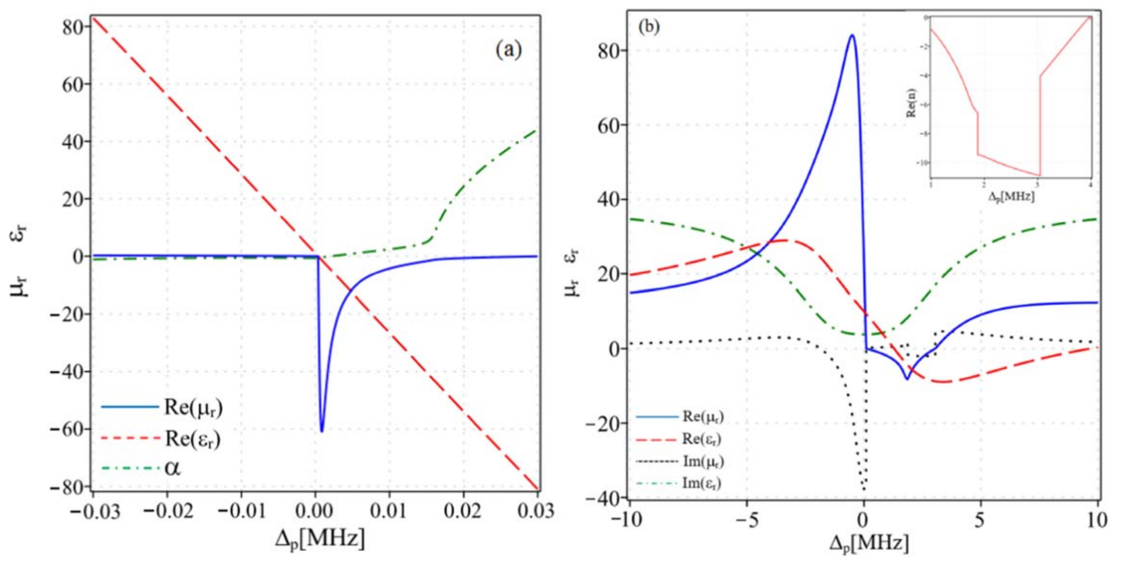

Figure 2. Plots of relative permittivity and relative permeability versus probe detuning in the absence (a) and the presence (b) of the Doppler broadening. The used parameters are $\Omega_c = 1$ MHz (a) and $\Omega_c = 60$ MHz (b), $\Delta_c = 0$ and T = 300 K. The insert shows the negative index of LHM.

Having the expressions of the electric and magnetic susceptibilies, the relative permittivity and relative permeability of the atomic medium are determined by

$$\varepsilon_r(D) = 1 + \chi_e(D), \tag{23}$$

$$\mu_r(D) = 1 + \chi_m(D). \tag{24}$$

Using expressions (23) and (24), the refractive index of a left-handed material can be given by:

$$n = -\sqrt{\varepsilon_r(D)\mu_r(D)}. \tag{25}$$

For a negative index material, the absorption coefficient can be expressed by [19]:

$$\alpha = -2\pi \mathrm{Im}(\sqrt{\varepsilon_r(D)\mu_r(D)}). \tag{26}$$

3. Results and discussion

We apply the calculation results to ^{87}Rb atom with selected states as $5S_{1/2}$ (F = 1), $5P_{1/2}$ (F′ = 2) and $5S_{1/2}$ (F = 2) corresponding to the levels $|1\rangle$, $|2\rangle$ and $|3\rangle$. The atomic density and other parameters used are $N = 10^{27}$ atoms/m^3, $m = 1.44 \times 10^{-27}$ kg, $d_{21} = 1.2 \times 10^{-29}$ C.m, $m_{31} = 7.26 \times 10^{-23}$ A.m^2, $\gamma_{21} = \gamma_{23} = 6$ MHz, $\varepsilon_0 = 8.85 \times 10^{-12}$ F m^{-1}, $\mu_0 = 4\pi \times 10^{-7}$ N A^{-2} and $k_B = 1.38 \times 10^{-23}$ J/K.

Firstly, in order to see the influence of Doppler broadening on negative refractive index we plot the real parts of relative permittivity (dashed line) and relative permeability (solid line) versus the probe laser detuning in the absence (a) and presence (b) of Doppler broadening as shown in figure 2. The used parameters of the coupling laser in figure 2 are $\Delta_c = 0$, $\Omega_c = 1$ MHz (a) and $\Omega_c = 60$ MHz (b), and T = 300 K. It should be noted that figure 2(a) is the same result as in [19] without Doppler broadening. From figure 2(a) we find that the real parts of permittivity (ε_r) and relative permeability (μ_r) are simultaneously negative in the frequency detuning range [0, 0.02 MHz], i.e., the medium exhibits left-handed property in the range [0, 0.02 MHz]. In particular, in this range, the medium has very small absorption (can see imaginary parts of ε_r and μ_r) due to the EIT effect established (see dash-dotted line). From figure 2(b) we also find that both of relative permittivity and relative permeability are simultaneously negative in the range [1.8 MHz, 3 MHz] and as a consequence the negative refractive index of the LHM is obtained in this range as depicted in the figure insert. We also note that the medium shows left-handedness only when both real ε_r and real μ_r are negative and the real part of refractive index (n) is negative [30], thus outside the range [1.8 MHz, 3 MHz] the medium does not exhibit left-handedness even though the real part of (n) is negative.

By comparing the results between figures 2(a) and (b) we see that the frequency band of negative refractive index with Doppler broadening is significantly expanded (about hundred times) compared to that without Doppler broadening. However, in order to achieve negative refractive index in the case of Doppler broadening, the coupling light intensity is approximately ten times greater than when Doppler broadening is ignored. In

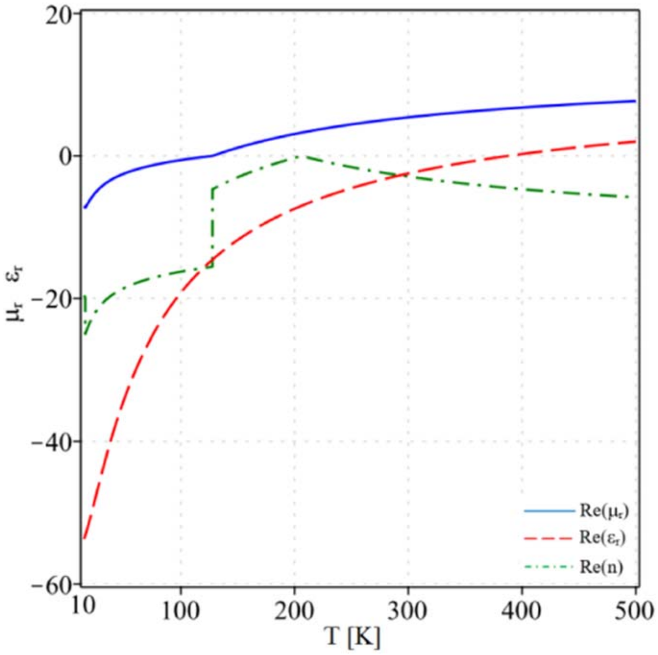

Figure 3. Real parts of relative permittivity (dashed line) and relative permeability (solid line) versus temperature at $\Delta_p = 2$ MHz, $\Delta_c = 0$ and $\Omega_c = 30$ MHz. The dash-dotted line is the refractive index of LMH.

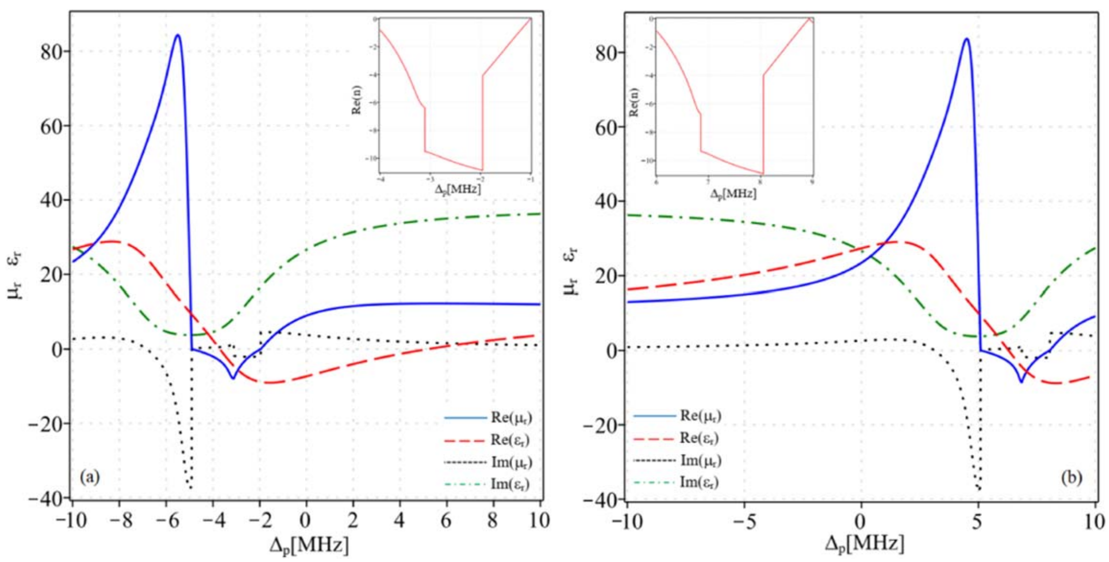

Figure 4. Plots of relative permittivity and relative permeability versus probe detuning for different values of coupling frequency detuning $\Delta_c = -5$ MHz (a) and $\Delta_c = 5$ MHz (b). The other parameters are $\Omega_c = 60$ MHz and T = 300K. The insert shows the negative index of LHM.

addition, in the presence of the Doppler broadening, the amplitudes of the relative permittivity and relative permeability are also reduced by about ten times compared when Doppler broadening absent. Even as the temperature increases, the left-handedness of the material can disappear as we see in figure 3. In figure 3 we plotted the relative permittivity and relative permeability, and the refractive index versus temperature at $\Delta_p = 2$ MHz, $\Delta_c = 0$ and $\Omega_c = 30$ MHz. In this case, the left-handedness of the material disappears when the temperature exceeds about 130 K. The physical reason for the above phenomena is due to the EIT effect is sensitively dependent on the temperature (Doppler width) of the atoms. As the temperature increases, the depth and width of the EIT window are markedly reduced, at the same time, the spectral profile is also significantly expanded [34]. Thus, to achieve the desired EIT efficiency (nearly 100%), the coupling laser intensity must also be much larger than the case without Doppler [34].

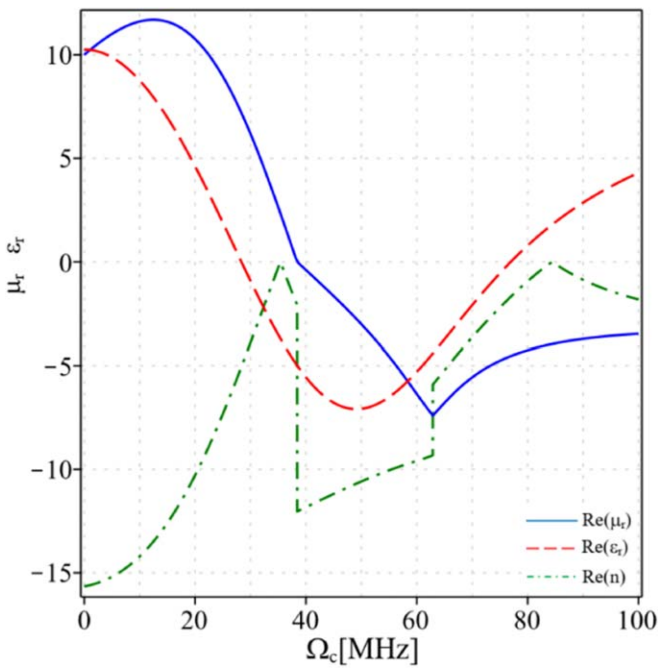

Figure 5. Real parts of relative permittivity (dashed line) and relative permeability (solid line) versus coupling Rabi frequency when $\Delta_p = 2$ MHz, $\Delta_c = 0$ and T = 300 K. The dash-dotted line is the refractive index of LMH.

Next, we show that the frequency range of the negative refractive index can be controlled according to the coupling laser frequency. To see this, in figure 4 we plotted the relative permittivity and the relative permeability, and the refractive index with respect to the probe laser detuning for different values of the coupling frequency detuning $\Delta_c = -5$ MHz (a) and $\Delta_c = 5$ MHz (b). It can see from figure 4 that the real parts of relative permittivity and relative permeability are simultaneously negative in the range [−3.2 MHz, −2 MHz] when $\Delta_c = -5$ MHz and in the range [6.8 MHz, 8 MHz] when $\Delta_c = 5$ MHz, and hence the negative refractive index of the LHM is also obtained in these ranges as we see in the insert. Thus, the frequency band of negative refractive index is shifted towards low frequency region when $\Delta_c = -5$ MHz and towards high frequency region when $\Delta_c = 5$ MHz. This is because when changing the coupling laser frequency around the atomic resonant frequency, the position of the EIT window (can see imaginary parts of ε_r and μ_r) is also changed according to the two-photon resonance condition [48], and thus the frequency range of the negative refractive index is shifted accordingly.

Finally, we fix the probe frequency detuning at $\Delta_p = 2$ MHz which corresponds to the negative refractive index region in figure 4, and study the influence of the coupling laser intensity on the negative refractive index. The graphs of relative permittivity and relative permeability, and the refractive index versus the coupling Rabi frequency when $\Delta_p = 2$ MHz, $\Delta_c = 0$ and T = 300 K are shown in figure 5. From figure we can see that both relative permittivity (dashed line) and relative permeability (solid line) varies from positive to zero then to negative when adjusting the coupling Rabi frequency from 0 to 100 MHz. It is because for a given frequency of the probe beam, a change in coupling laser intensity can lead to a transition between electromagnetically induced transparency (EIT) and electromagnetically induced absorption (EIA) [48] which changes the corresponding dispersion properties. In this case, we also find the medium shows left-handedness when 38 MHz $< \Omega_c <$ 78 MHz.

4. Conclusion

We have derived the expressions of the relative permittivity and the relative permeability in the Doppler broadened three-level Λ-type atomic medium. We have found that under the EIT condition, the negative refractive index of the medium have achieved in an optical frequency band. In the presence of Doppler broadening, the conditions for achieving negative refractive index are very different from those of Doppler broadening absent. In particular, with Doppler broadening the coupling laser intensity must be tens of times approximately greater than that without Doppler broadening. The frequency band of negative refractive index with Doppler broadening is expanded about a hundred times larger than that without Doppler broadening, while the amplitude of negative refractive index decreases with increasing temperature. Even when increasing temperature (Doppler width), the left-handedness of the material can disappear. In addition, the frequency band of negative refractive index can be changed by varying the coupling laser frequency, while the amplitude of negative refractive index can be controlled by adjusting the coupling laser intensity.

Acknowledgments

The authors are grateful to the editor and the referees for their valuable comments and constructive suggestions, which have contributed to the final preparation of the paper. Research was supported by Vietnamese National Foundation of Science and Technology Development (Grant No. 103.03-2019.383).

Data availability statement

No new data were created or analysed in this study.

ORCID iDs

Nguyen Huy Bang https://orcid.org/0000-0003-4702-3157
Le Van Doai https://orcid.org/0000-0002-1850-3437

References

[1] Veselago V G 1968 The electrodynamics of substances with simultaneously negative values of ε and μ *Sov. Phys. Usp.* **10** 509
[2] Smith D R, Padilla W J, Vier D C, Nemat-Nasser S C and Schultz S 2000 Composite medium with simultaneously negative permeability and permittivity *Phys. Rev. Lett.* **84** 4184–7
[3] Shelby R A, Smith D R and Schultz S 2001 Experimental verification of a negative index of refraction *Science* **292** 77–9
[4] Pendry J B 2000 Negative refraction makes a perfect lens *Phys. Rev. Lett.* **85** 3966
[5] Chen L, He S and Shen L 2004 Finite-size effects of a left-handed material slab on the image quality *Phys. Rev. Lett.* **92** 107404
[6] Aydin K, Bulu I and Ozbay E 2007 Subwavelength resolution with a negative-index metamaterial superlens *Appl. Phys. Lett.* **90** 254102
[7] Lakhtakia A 2004 Positive and negative goos-hänchen shifts and negative phase-velocity mediums (alias left-handed materials) *Int. J. Electron. Commun. (AEU)* **58** 229
[8] Williams J M 2001 Some problems with negative refraction *Phys. Rev. Lett.* **87** 249703
[9] Yang Y P, Xu J P, Chen H and Zhu S Y 2008 Quantum interference enhancement with left-handed materials *Phys. Rev. Lett.* **100** 043601
[10] Yannopapas V, Paspalakis E and Vitanov N V 2008 Plasmon-induced enhancement of quantum interference near metallic nanostructures *Phys. Rev. Lett.* **103** 063602
[11] Pendry J 2003 Positively negative *Nature* **423** 22–3
[12] Cubukcu E, Aydin K, Ozbay E, Foteinopoulou S and Soukoulis C M 2003 Electromagnetic waves: negative refraction by photonic crystals *Nature* **423** 604
[13] Eleftheriades G V, Iyer A K and Kremer P C 2002 Planar negative refractive index media using periodically L-C loaded transmission lines *IEEE Trans. Microwave Theory Tech.* **50** 2702
[14] Yannopapas V 2006 Negative index of refraction in artificial chiral materials *J. Phys. Condens. Matter* **18** 6883
[15] Li Z, Mutlu M and Ozbay E 2013 Chiral metamaterials: from optical activity and negative refractive index to asymmetric transmission *J. Opt.* **15** 023001
[16] Boller K J, Imamoglu A and Harris S E 1991 Observation of electromagnetically induced transparency *Phys. Rev. Lett.* **66** 2593
[17] Javanainen J 1992 Effect of state superpositions created by spontaneous emission on laser-driven transitions *Europhys. Lett.* **17** 407
[18] Oktel M O and Mustecaplioglu O E 2004 Electromagnetically induced left-handedness in a dense gas of three-level atoms *Phys. Rev. A* **70** 053806
[19] Shen J Q, Ruan Z C and He S 2004 How to realize a negative refractive index material at the atomic level in an optical frequency range *J. Zhejiang Univ. Science* **5** 1322
[20] Krowne C M and Shen J Q 2009 Dressed-state mixed-parity transitions for realizing negative refractive index *Phys. Rev. A* **79** 023818
[21] Thommen Q and Mandel P 2006 Electromagnetically induced left handedness in optically excited four-level atomic media *Phys. Rev. Lett.* **96** 053601
[22] Zhang H J, Niu Y P and Gong S Q 2007 Electromagnetically induced negative refractive index in a V-type four-level atomic system *Phys. Lett. A* **363** 497
[23] Zhao S C, Liu Z D and Wu Q X 2010 Left-handedness without absorption in the four-level Y-type atomic medium *Chin. Phys. B* **19** 014211
[24] Zhao S C, Liu Z D and Wu Q X 2010 Negative refraction without absorption via both coherent and incoherent fields in a four-level left-handed atomic system *Opt. Comm.* **283** 3301–4
[25] Zhao S C, Liu Z D and Wu Q X 2010 Zero absorption and a large negative refractive index in a left-handed four-level atomic medium *J. Phys. B: At. Mol. Opt. Phys.* **43** 045505
[26] Zhang Z Q, Liug Z D, Zhao S C, Zheng J, Ji Y F and Liu N 2011 Negative refractive index in a four-level atomic system *Chin. Phys. B* **20** 124202
[27] Othman A and Yevick D 2016 Enhanced negative refractive index control in a 5-level system *J. Mod. Opt.* **64** 1208–14
[28] Ba N, Gao J W, Fan W, Wang D W, Ma Q R, Wang R and Wu J H 2008 Electromagnetically induced negative refraction in an atomic system with spontaneously generated coherence *Opt. Comm.* **281** 5566–70
[29] Dutta S and Dastidar K R 2010 Realization of a negative refractive index in a three-level Λ system via spontaneously generated coherence *J. Phys. B: At. Mol. Opt. Phys.* **43** 215503

[30] Osman K I and Joshi A 2012 Left-handedness in K-type multilevel system in the presence of spontaneously generated coherence *Opt. Comm.* **285** 3162–8
[31] Li Y Q and Xiao M 1995 Electromagnetically induced transparency in ladder-type inhomogeneously broadened media: Theory and experiment *Phys. Rev. A* **51** 576–84
[32] Zhang L, Zhou F, Niu Y, Zhang J and Gong S 2011 The effect of doppler broadening on dispersive and absorptive properties in atomic systems with two-photon interference *Opt. Comm.* **284** 5697–701
[33] Mitra S, Dey S, Hossain M M, Ghosh P N and Ray B 2013 Temperature and magnetic field effects on the coherent and saturating resonances in Λ- and V-type systems for the 85Rb-D2 transition *J. Phys. B: At. Mol. Opt. Phys.* **46** 075002
[34] Khoa D X, Trong P V, Doai L V and Bang N H 2016 Electromagnetically induced transparency in a five-level cascade system under Doppler broadening: an analytical approach *Phys, Scr.* **91** 035401
[35] Kaur P, Bharti V and Wasan A 2017 Optical properties of an inhomogeneously broadened multilevel V-system in the weak and strong probe regimes *Ind. J. Phys.* **91** 1115–25
[36] Khoa D X, Trung L C, Thuan P V, Doai L V and Bang N H 2017 Measurement of dispersive profile of a multi-window EIT spectrum in a Doppler-broadened atomic medium *J. Opt. Soc. Am. B* **34** 1255–63
[37] Zhang G, Tao Q, Zhao Z and Ren Z 2017 Effect of thermal motion on the phenomenon of electromagnetically induced transparency *Optik* **138** 153–9
[38] Ali H, Ziauddin and Ahmad I 2014 The effect of Kerr nonlinearity and Doppler broadening on slow light propagation *Laser Phys.* **24** 025201
[39] Bharti V and Natarajan V 2017 Sub- and super-luminal light propagation using a Rydberg state *Opt. Comm.* **392** 180–4
[40] Katz O and Firstenberg O 2018 Light storage for one second in room-temperature alkali vapor *Natute Comm.* **9** 2047
[41] Anh N T, Doai L V, Son D H and Bang N H 2018 Manipulating multi-frequency light in a five-level cascade EIT medium under Doppler broadening *Optik* **171** 721–7
[42] Li L and Huang G 2010 Linear and nonlinear light propagations in a Doppler-broadened medium via electromagnetically induced transparency *Phys. Rev. A* **82** 023809
[43] Khoa D X, Dong H M, Doai L V and Bang N H 2017 Propagation of laser pulse in a three-level cascade inhomogeneously broadened medium under electromagnetically induced transparency conditions *Optik* **131** 497–505
[44] Wang H, Goorskey D and Xiao M 2001 Enhanced Kerr nonlinearity via atomic coherence in a three-level atomic system *Phys.Rev.Lett.* **87** 073601
[45] Sheng J, Yang X, Wu H and Xiao M 2011 Modified self-Kerr-nonlinearity in a four-level N-type atomic system *Phys. Rev. A* **84** 053820
[46] Bang N H, Khoa D X, Son D H and Doai L V 2019 Effect of Doppler broadening on giant self-Kerr nonlinearity in a five-level ladder-type system *J. Opt. Soc. Am. B* **36** 3151
[47] Bang N H, Khoa D X and Doai L V 2020 Controlling self-Kerr nonlinearity with an external magnetic field in a degenerate two-level inhomogeneously broadened medium *Phys. Lett. A* **384** 126234
[48] Bang N H, Doai L V and Khoa D X 2019 Controllable optical properties of multiple electromagnetically induced transparency in gaseous atomic media Comm *Phys.* **29** 1–33